Supporting Information for:

Electron Transfer and Proton-Coupled Electron Transfer Reactivity and Self-Exchange of Synthetic [2Fe-2S] Complexes: Models for Rieske and mitoNEET Clusters

Caroline T. Saouma, Margaux M. Pinney, James M. Mayer*

Table of Contents

A. General Considerations

Unless noted, all manipulations were carried out using standard Schlenk or glove-box techniques under a dinitrogen atmosphere. Glassware was oven-dried for 24 h prior to use. Celite and molecular sieves were dried by heating to 300 ^{o}C under vacuum for 24 h. Unless otherwise noted, solvents were deoxygenated and dried by sparging with Ar followed by passage through Grubbs-style columns filled with activated alumina.[1] Tetrahydrofuran was further dried by stirring over sodium/benzophenone and vac-transferring. Acetonitrile was purchased from Burdick and Jackson® (< 5ppm low-water brand) and stored in an Ar pressurized stainless steel drum plumbed directly into a glove-box. Dimethylformamide was degassed and dried over activated 3 Å molecular sieves. Nonhalogenated solvents were tested with a standard purple solution of benzophenone ketyl in THF to confirm effective oxygen and moisture removal, and all glove-box solvents were stored over activated 3 Å molecular sieves. Deuterated solvents were purchased from Cambridge Isotopes Laboratories, Inc. and were degassed and stored over activated 3 Å molecular sieves prior to use. d_3-MeCN was dried over CaH_2 and vac-transferred prior to storage over sieves. Methanol was degassed and stored over activated 3 Å molecular sieves.

B. Spectroscopic Measurements

NMR spectra were collected on Bruker 500 MHz spectrometers, and ^{1}H chemical shifts were referenced to residual solvent. MestReNova (8.1.2) was used for NMR data workup.

EPR spectra were collected on a Bruker EMX CW X-band spectrometer outfitted with a cryo-cooled cavity. Spectra were collected in a 1:2 MeCN:toluene glass (~ 1 mM) at 127 K at 9.287 GHz (the attenuator was 15.0 dB). The receiver gain was set to 2.24×10^{5} with a modulation amplitude of 5 G (the modulation frequency was set to 100 kHz). The time constant and conversion time were set to 10.24 ms and 40.96 ms, respectively. EPR spectra were simulated using the W95EPR program.[2] The derivative curves were fit to a Gaussian.

Optical spectroscopy measurements were taken on a Hewlett-Packard 8453 diode array spectrophotometer equipped with a Unisoku sample holder that has a temperature controller and magnetic stirrer. Unless noted, all optical spectroscopy measurements were done in MeCN. Samples were taken using quartz cuvettes sealed to a Teflon valve (Kontes) and 14/20 ground-glass joint. For stability studies of **5**, in the glove-box, solutions of **2** were loaded into the cuvette with a stir bar, and the solution exposed to dynamic vacuum (~ 10 s) prior to closing the valve. Solutions of [DMAP-H]OTf were added to the side-arm between the Kontes valve and the 14/20 joint, which was then capped with a greased 14/20 glass stopper. The assembly was then removed from the glove-box. After the spectrum of **2** was obtained, the valve was opened, allowing mixing of the acid solution with that of **2**. UV-vis spectra were then collected every 60 s.

C. Rapid Kinetics Measurements

Rapid kinetic measurements were taken using a HI-TECH SCIENTIFIC CryoStopped-Flow System (SF-61DX2) capable of double-mixing, and equipped with a TC-61 temperature controller and a diode array detector. The stopped-flow system was controlled by the Kinetic

Studio 2.20 software. The system was thermally equilibrated for 30-60 min before data acquisition at each temperature, and prior to kinetic runs, the stopped-flow was thoroughly flushed with dry MeCN.

All volumetric glassware and glass syringes employed were rinsed with dry MeCN in the glove-box prior to use. Reagents and MeCN were loaded into gas-tight syringes (Hamilton or SGE), which were attached to gas-tight 2-way valves (SGE). The syringes were placed into individual Ziploc bags filled with glove-box atmosphere, removed from the glove-box, and immediately attached to the stopped-flow. The individual stopped-flow lines were rinsed with reagent prior to shots. The first two shots of every temperature/concentration combination were omitted.

Kinetic data were analyzed using ReactLab KINETICS (1.1) by global fitting of all wavelengths. For *pseudo*-first-order kinetics, the linear regression of k_{obs} versus [TEMPO] and the Eyring plot was done in Kaleidagraph, weighting each rate constant with its associated standard deviation. Standard errors were obtained from the plots, which were converted to standard deviation. Unless noted, reported errors are double the fully propagated standard deviations, except that of the activation entropy, which is quadruple the fully propagated standard deviation.

D. Starting Materials and Reagents

Reagents were purchased from Aldrich and unless noted, used without further purification. 4-Dimethylaminopyridine (DMAP) was crystallized from toluene.[3] $CoCp^*_2$ was purified by dissolution into pentane, filtering through a Celite-lined frit, and removal of pentanes. TEMPO (2,2,6,6-tetramethylpiperidin-1-yl-oxyl) was sublimed under vacuum.[3] TEMPOH was prepared as described in the literature,[4] and further purified by dissolution into minimal Et_2O, removal of the water which separated out, pumping down to a solid, and sublimation (2x). $^nBu_4NPF_6$ was triply crystallized from EtOH/MeCN and subsequently dried under vacuum for 48 h at 50 ^oC. [DMAP-H]OTf, and [pyH]OTf were prepared by addition of 1 equiv triflic acid to the corresponding base in Et_2O. The resulting precipitates were isolated, and recrystallized from MeCN. [DMAP-D]OTf was prepared analogously using DOTf. Clusters **1**, **2**, **3**, **4**,[5] and $[Fe_2S_2(SArO)_2]^{2-/3-}$ were prepared as previously described.[6]

E. Generation of [Fe₂S₂(^Prbbim H₂)(^Prbbim)](Et₄N), 5

A 5.7 mM solution of **2** in d_3-MeCN (0.6 mL, 3.4 μmol) was prepared and transferred to an NMR tube that was capped with a rubber septum and parafilmed. The NMR tube was chilled in an *o*-xylenes/dry ice cold bath. To this, 100 μL of a 68 mM solution of [DMAP-H]OTf in d_3-MeCN (6.8 μmol) was added via gas-tight syringe. The NMR tube was immediately inverted 3 times to ensure full mixing and kept cold. Cluster **5** is not thermally stable, decomposing in seconds to minutes (at room temperature) to MeCN-insoluble species. ^1H NMR (MeCN-d_3, 500 MHz, –20 ^oC): δ 20.8 (bs), 12.9 (bs), 2.93 (Et_4N^+), 1.06 (Et_4N^+). UV-vis (MeCN, 25 ^oC, 0.01s after mixing **2** + 2 equiv [DMAP-H]OTf via stopped-flow) λ_{max}, nm (ε, M^{-1} cm^{-1}): 527 (2500), 578 (1600). X-band EPR (9.287 GHz, 127 K, 1:2 MeCN:toluene): g = [1.990, 1.950, 1.885], W = [65, 40, 60 G].

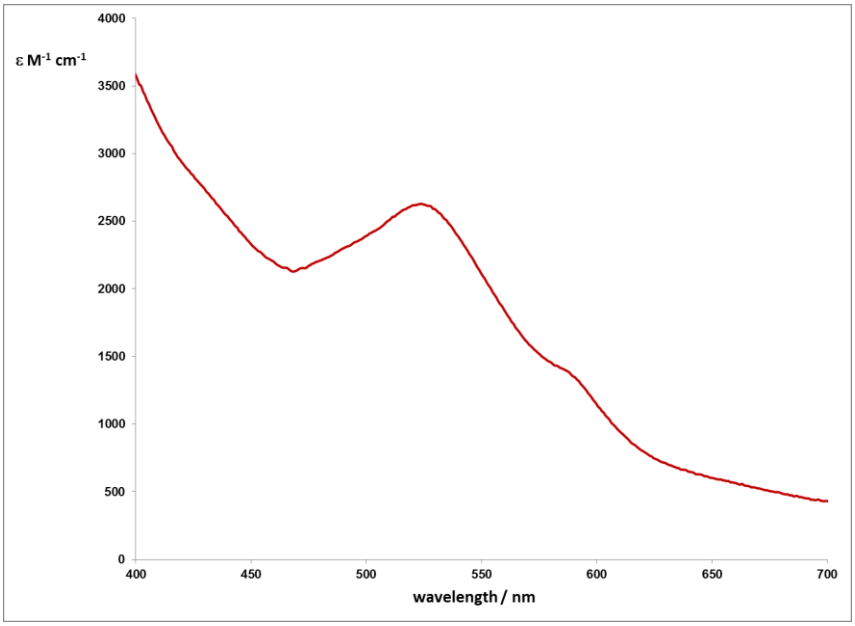

Figure S1. UV-vis spectrum of **5** in MeCN.

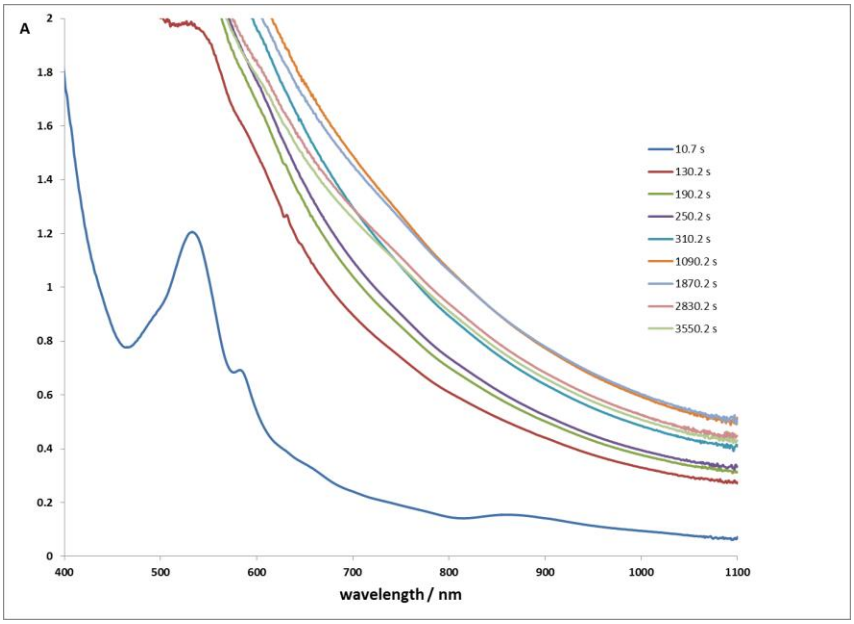

Figure S2. Stacked UV-vis spectra for the decomposition of **5** at 25 ^{o}C in MeCN (**5** was generated by addition of 290 μL of a 14.4 mM solution of [DMAP-H]OTf to 4 mL of a 0.51 mM solution of **2**.

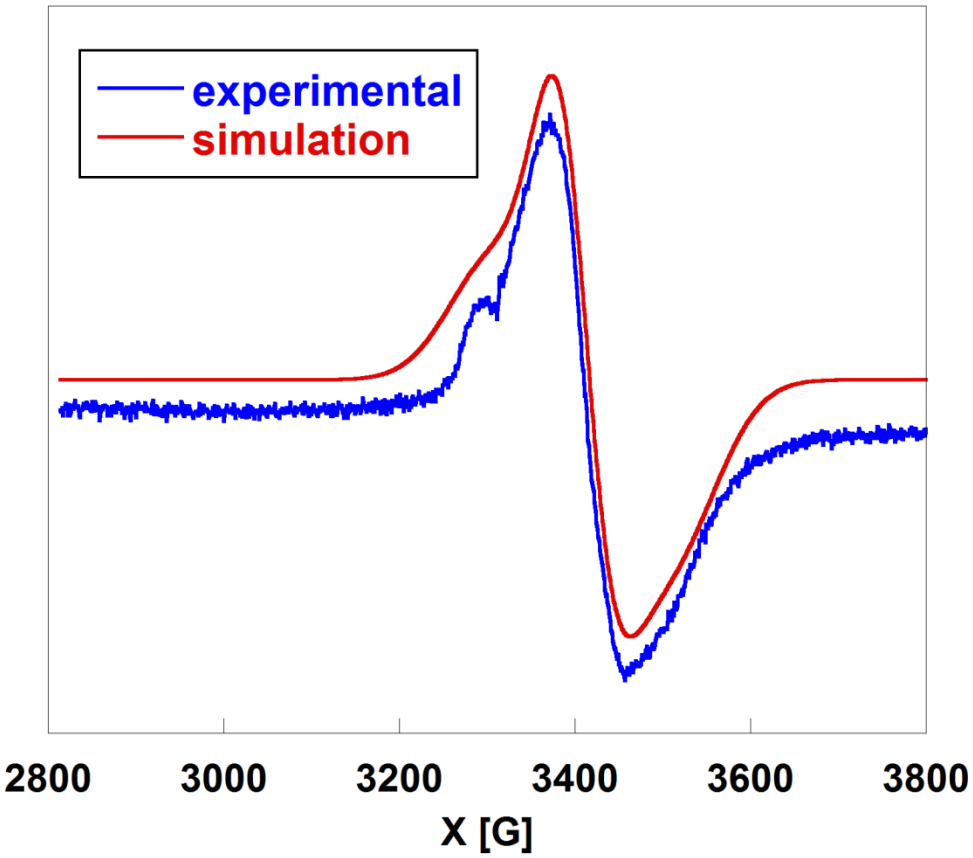

Figure S3. EPR spectrum of **5** obtained at 127 K in a 1:2 MeCN:toluene glass. The spectrum was fit using Gaussian lineshapes to give g = [1.990, 1.950, 1.885], W = [65, 40, 60 G].

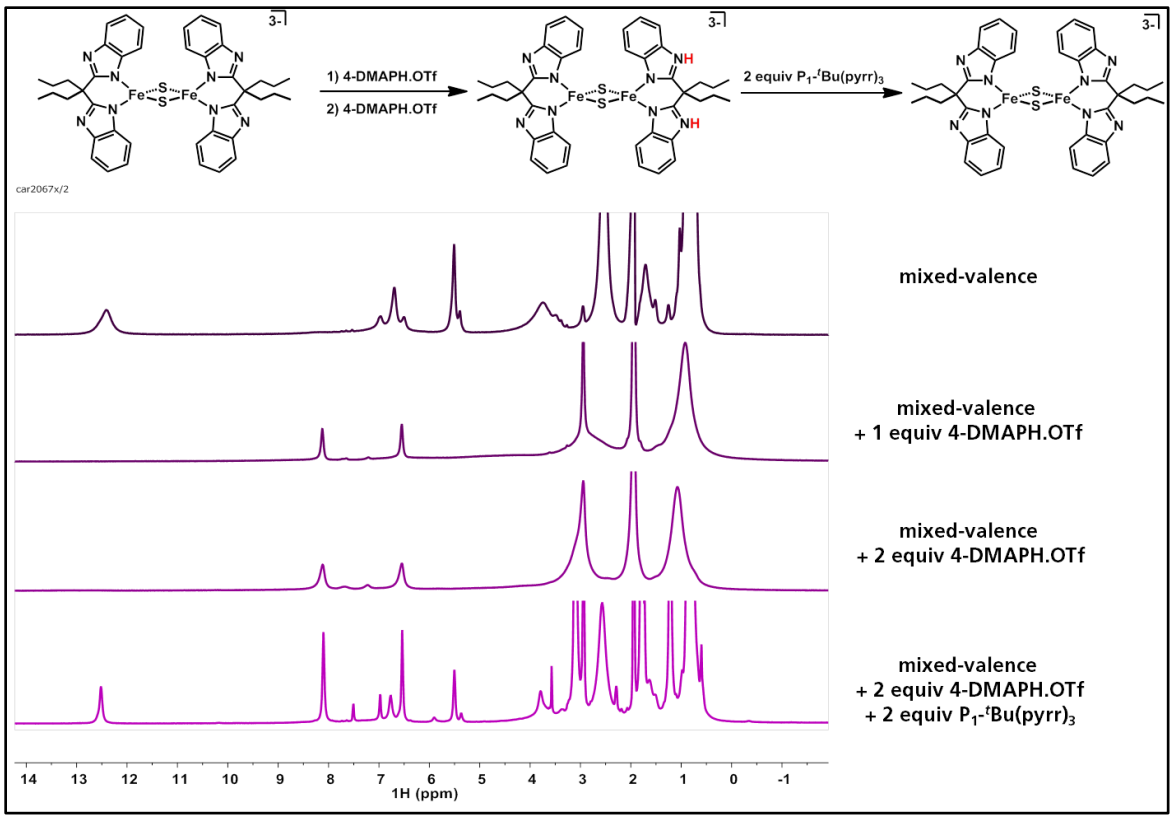

Figure S4. Stacked ^{1}H NMR spectra (MeCN-d_3, -20 ^{o}C) of (top): **2**; (middle): addition of 1 and 2 equiv [DMAP-H]OTf to generate **4** and **5**, respectively; (bottom): addition of 2 equiv of ^{t}BuN=P(pyrr)$_3$ to regenerate **2**. Integration of the peak at 12.52 of **2** relative to the peaks of DMAP suggests ~75 % conversion back to **2**.

F. Self-Exchange Kinetics

F.I PT Self-Exchange Kinetics for 1 and 3

1 mL aliquots of solutions of **1** (1.94 mM) in d_3-MeCN were transferred to five NMR tubes and capped with rubber septa and sealed with parafilm (in the glove-box). At the NMR spectrometer, 0, 16, 32, 48, or 64 μL of a 30 mM solution of [pyH]OTf in d_3-MeCN was added to each tube, inverted twice, and inserted in the probe (corresponding to 0, 0.25, 0.5, 0.75, or 1 equiv of acid). The linewidth of the resonance ascribed to the proton at the 4 position of the ligand benzimidazolate was obtained by peak fitting to a Lorentzian using MestReNova 8.1.2., which gave the line widths (full width at half-maximum): W_1 = 18.2 Hz and W_3 of 25.9 Hz.

NMR spectra of mixtures of **1** and **3** in d_3-MeCN show a single set of ligand resonances, which shift according to the mole fraction of **1** and **3**. This indicates of rapid intermolecular PT exchange between **1** and **3** on the NMR timescale. Assuming a simple 2-site exchange system comprised of **1** and **3**, and that the rate law for PT is first order with respect to each reactant

concentration, then rate of PT can be obtained from the following[7] $W_{13} = \chi_1 W_1 + \chi_3 W_3 + \frac{4\pi\chi_1\chi_3(\Delta\upsilon)^2}{k_6 C_{13}}$. In this equation, W_{13}, W_1, and W_3 are line widths for a given resonance in mixtures of **1**+**3**, **1**, and **3**, χ_1 and χ_3 are the mole fractions of **1** and **3**, C_{13} is the total molar concentration of **1** and **3**, $\Delta\nu$ is the chemical shift difference between **1** and **3**, and k_3 is the rate of PT between **1** and **3**. Unfortunately, W_{13} is not substantially larger than the sum $\chi_1 W_1 + \chi_2 W_2$, so the rate of intermolecular PT cannot accurately be determined. Instead, we simply assume that the rate constant must be larger than that at the coalescence temperature ($k_{obs} = \frac{\pi\delta\nu}{\sqrt{2}}$).[8] Despite the small chemical shift difference, $\delta\nu >> (\pi T_2)^{-1}$ (T_2 taken as the linewidth of **1** and **3**), making this equation valid. This gives a first-order rate constant of 66 s^{-1}. For ~ 2 mM solutions, this corresponds to a second-order rate constant of ~ 10^4 M^{-1} s^{-1} at the coalescence temperature.

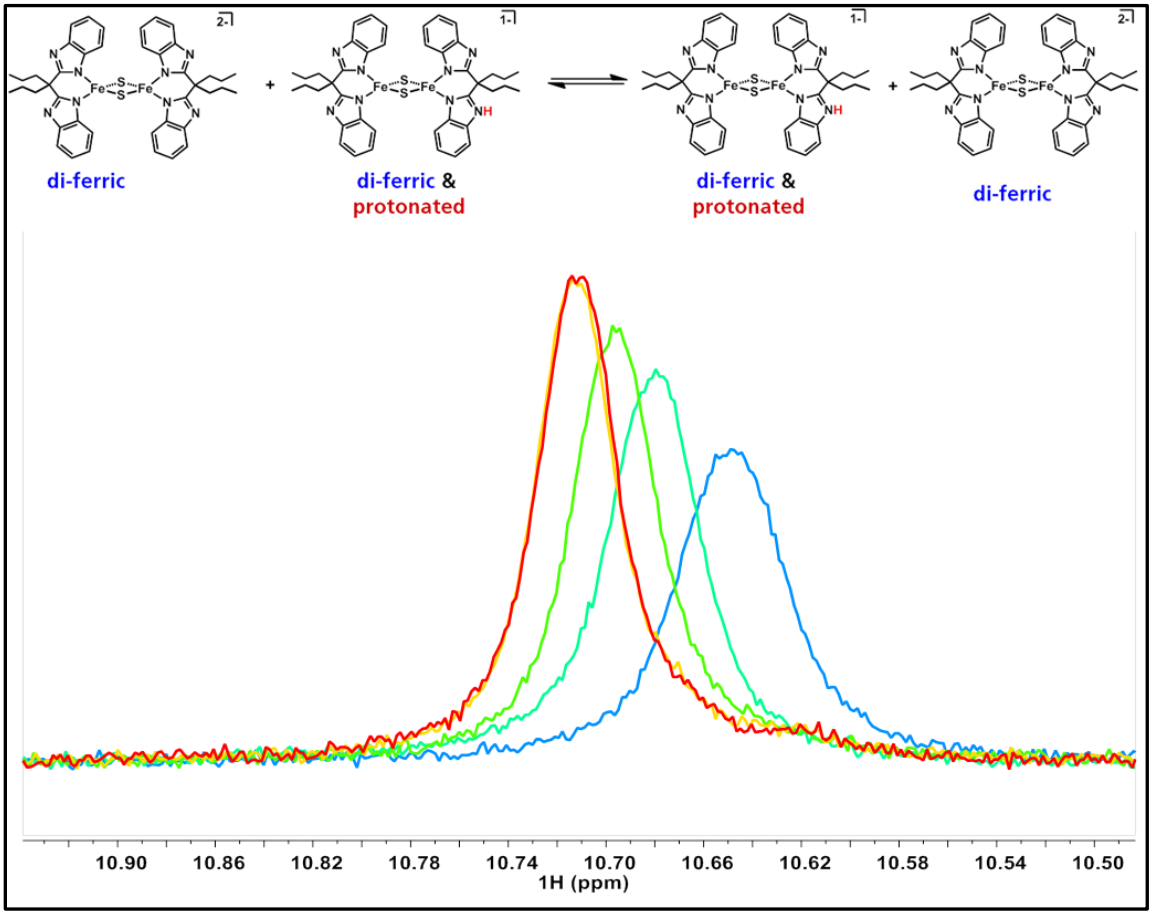

Figure S5. Overlaid ^{1}H NMR spectra (MeCN-d_3, 25 ^{o}C) of (red): **1**; (orange): 3:1 **1**:**3**; (green): 1:1 **1**:**3**; (green-blue): 1:3 **1**:**3**; (blue): **3**.

F.II PT Self-Exchange Kinetics for 2 and 4

In the glove-box, 600 μL of a 5.7 mM solution of **2** in d_3-MeCN was transferred to an NMR tube which was capped with a rubber septum and parafilmed. Also in the glove-box, a solution of [DMAP-H]OTf in d_3-MeCN (68 mM) was prepared and transferred to a vial containing a septum screwcap which was then parafilmed. A 50 μL gas-tight syringe was inserted via the septum, as well as a 10 mL disposable syringe full of glove-box atmosphere (to keep the solution under inert atmosphere). The ^{1}H NMR spectrum of the solution of **2** was collected at – 20 ^{o}C. The sample was removed from the probe, and while the tube was chilled in an *o*-xylenes/dry ice cold bath, 10 μL of the acid solution (0.2 equiv) was added via syringe. The sample was inverted twice prior to insertion into the chilled NMR probe. The NMR spectrum was then collected. To a second identical sample of **2**, 25 μL of the acid solution was added analogously, and the NMR spectrum obtained. The linewidth of the resonance ascribed to the proton at the 4 position of the ligand benzimidazolate was obtained by peak fitting to a Lorentzian using MestReNova 8.1.2. The rate of intermolecular PT between **2** and **4** was estimated from eq 8 of the main text using linewidths from the sample of **2** and **2** + 0.2 equiv acid. The resonance was too broad to observe when 0.5 equiv of acid was added to **2**. See Figure S6.

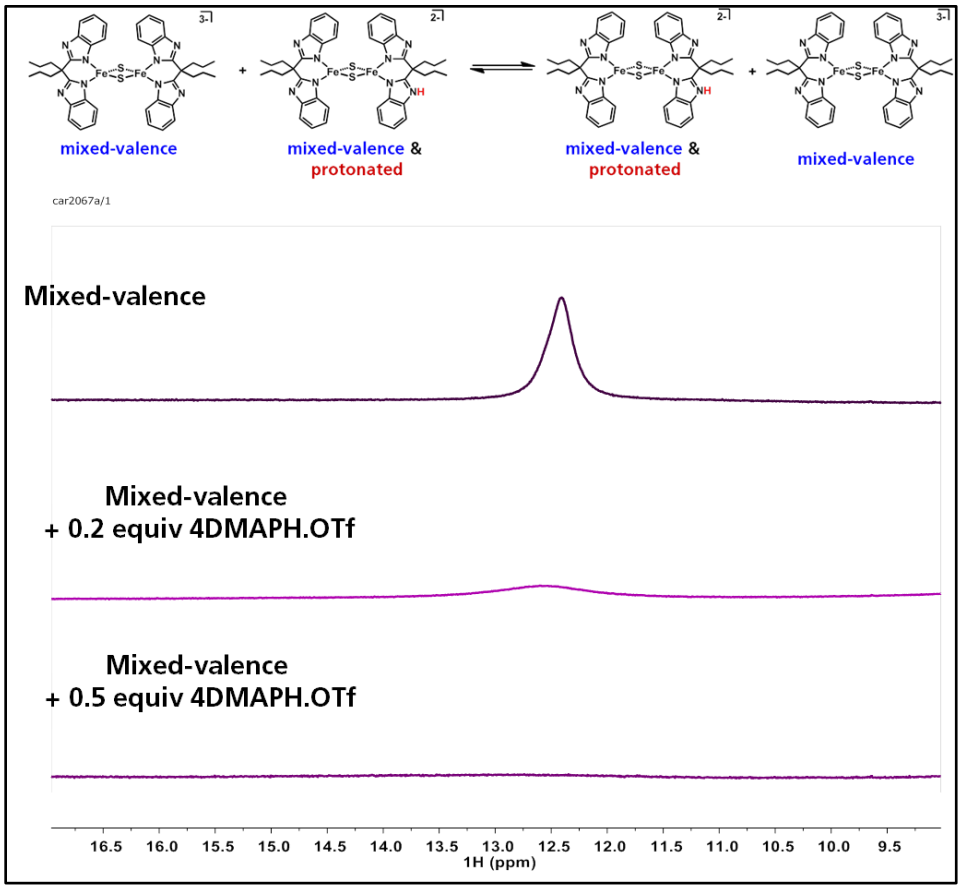

Figure S6. Stacked ^{1}H NMR spectra (MeCN-d_3, - 20 ^{o}C) of (top): **2**; (middle): **2** + 0.2 equiv acid; (bottom): **2** + 0.5 equiv acid. From the broadening, the rate constant for intermolecular PT between **2** and **4** is estimated to be ~ 9×10^5 M^{-1} s^{-1}.

F.III ET Self-Exchange Kinetics for 1 and 2

In a glove-box, 2 mM solutions of **1** and **2** in d_3-MeCN were prepared. Mixtures of these solutions were aliquoted out into six NMR tubes to give samples with varying di-ferric to mixed-valence ratios (100:0, 85:15, 70:30, 55:45, 40:60, 0:1). The tubes were capped and parafilmed. Samples were recorded on a Bruker 500 MHz instrument (with no spinning) at 299, 268, 257, and 239 K. Each sample was allowed to thermally equilibrate in the probe for 5 minutes, after which the instrument was tuned and the shims adjusted. A methanol standard was used to confirm the temperature. In MestReNova, each spectrum was phased and baseline corrected. The "Fit Region" function was used to fit the resonance of the proton at the 4 position of the benzimidazolate of **1** to a Lorentzian and to extract the peak width. This resonance was chosen because it is well separated from all other resonances. The rate of intermolecular ET between **1** and **2** was obtained from the slope of the plot of [**2**] vs. $\pi\Delta W$. The linear regression of $\pi\Delta W$ versus [**2**] and the Eyring plot was done in Kaleidagraph, weighting each rate constant with its associated standard deviation for the Eyring plot. Standard errors were obtained from the plots, which were converted to standard deviation.

This method was repeated with electrolyte included. In a glove-box, 2mM solutions of **1** and **2** were prepared with d_3-MeCN that contained 6.0 mM $^n Bu_4NPF_6$. Mixtures of these solutions were aliquoted into NMR tubes with varying di-ferric to mixed-valence ratios (100:0, 90:10, 80:20, 70:30, 60:40). Samples were recorded on a Bruker 500 MHz instrument at 299 K in the manner discussed above. The spectra were modified and fit in MestReNova, as stated above, and a plot of $\pi\Delta W$ vs. [**2**] was obtained.

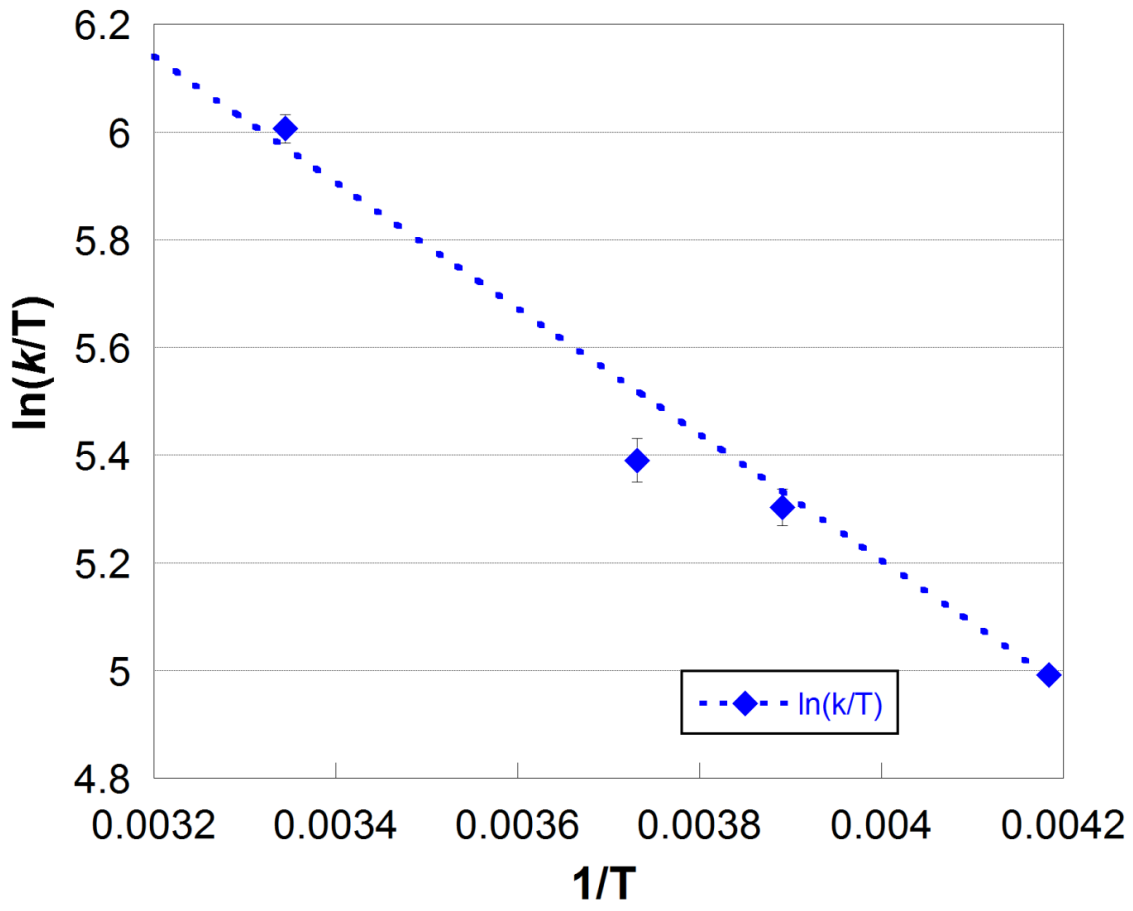

Figure S7. Eyring plot for intermolecular ET between **1** and **2** in d_3-MeCN.

F.IV Attempt to Measure ET Self-Exchange Kinetics for 3 and 4

In the glove-box, 2.0 mM solutions of **1** and **2** were prepared in d_3-MeCN, as was a 24.0 mM solution of [NH_4]OTf. Aliquots of **1** and **2** were transferred to five NMR tubes in varying ratios, with the total volume being 600 μL. 1 equiv of acid (50 μL) was added to each sample, as described above for PT kinetics of **1** and **3**. NMR spectra were collected at 243 K, and are shown in Figure S8. Similar spectra are obtained when [DMAP-H]OTf is employed as the acid. From the chemical shift of the protons at the 4 position of the benzimidazolates, the mole fraction of each species (**1** and **3**) can be determined. In Figure S8, the chemical shift in 70:30, 55:45, and 40:60 mixtures of di-ferric: mixed-valence indicate that no **3** is present in solution (**1** is the only di-ferric species). The chemical shift in the 85:15 mixture (Figure S8), indicates a mixture of **1** and **3**, which results from net ~ 3 protons transferred to each mixed-valence & protonated cluster, which is NMR silent (total of 4 protons).

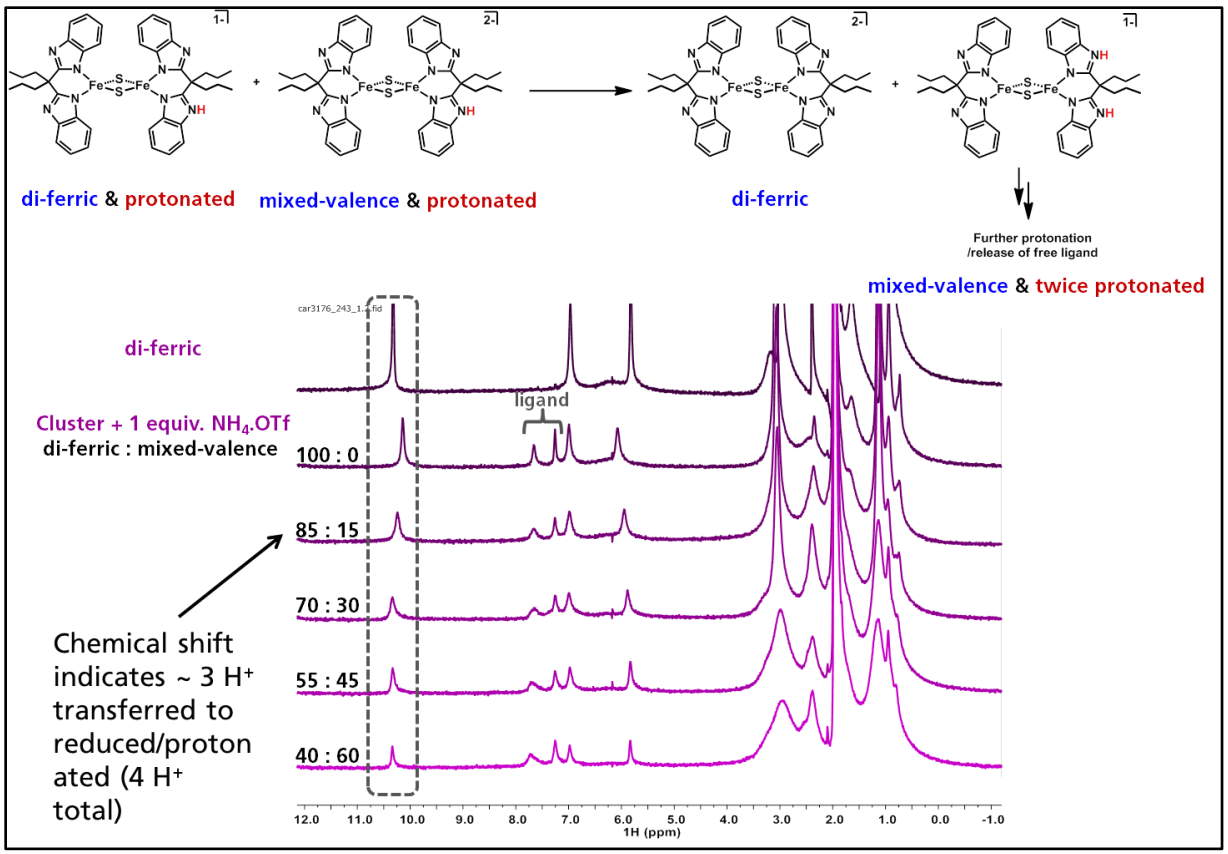

Figure S8. Stacked ^{1}H NMR spectra (MeCN-d_3, -30 ^{o}C) of **1** (top), and mixtures of **1** and **2** with 1 equiv. NH_4.OTf.

F.V ET Self-Exchange Kinetics for $[Fe_2S_2(SArO)_2](PPN)_2$/$[Fe_2S_2(SArO)_2](PPN)_2(CoCp^*_2)$

In a glove-box, solutions of $[Fe_2S_2(SArO)_2](PPN)_2$ (2.5 mM) and $CpCp^*_2$ (7.5 mM) were prepared in d_3-MeCN. 600 μL of the $[Fe_2S_2(SArO)_2](PPN)_2$ solution was aliquoted into six NMR tubes using a 1000 μL pipetteman. These aliquots were diluted with d_3-MeCN and/or $CpCp^*_2$ solution (200 μL total, 1.9 mM final concentration of cluster) to give samples with varying di-ferric to mixed-valence ratios (100:0, 70:30, 55:45, 40:60, 20:80, 0:100). The NMR tubes were immediately capped, inverted twice, parafilmed, and frozen with liquid nitrogen (outside of the glove-box). This latter step was done to minimize degradation of the mixed-valence cluster. Each sample was thawed at the NMR probe, and allowed to temperature equilibrate in the probe for 5 minutes, after which the instrument was tuned and the shims adjusted. In MestReNova, each spectrum was phased and baseline corrected. The "Fit Region" function was used to fit the resonances to a Lorentzians and to extract the peak width.

Both the mixed-valence and di-ferric cluster congeners in this system have four well-defined resonances that correspond to the 4 distinct protons of the thiosalicylate ligand. However, each of the four resonances for the di-ferric cluster are split into two (~ 4:6), suggesting that both the *cis* and *trans* isomers are present in solution. The four resonances for the mixed-valence congener can be fit to single Lorentzians, indicating that if both isomers are

present in solution, interconversion is fast on the NMR timescale. For the line broadening analysis, both the resonance at 4.00 ppm of the di-ferric cluster and that at 3.06 ppm for the mixed-valence congener were analysed. These resonances were chosen because they are well-isolated from the other resonances, and in the case of the resonance of the di-ferric cluster, the difference in chemical shift for the two isomers is minimal (~ 10 Hz). Both resonances were fit to single Lorentzian curves. The assumption that both resonances correspond to a single Lorentzian, and/or the presence of a paramagnetic impurity may contribute to the poor fit of the plot depicted in Figure S11.

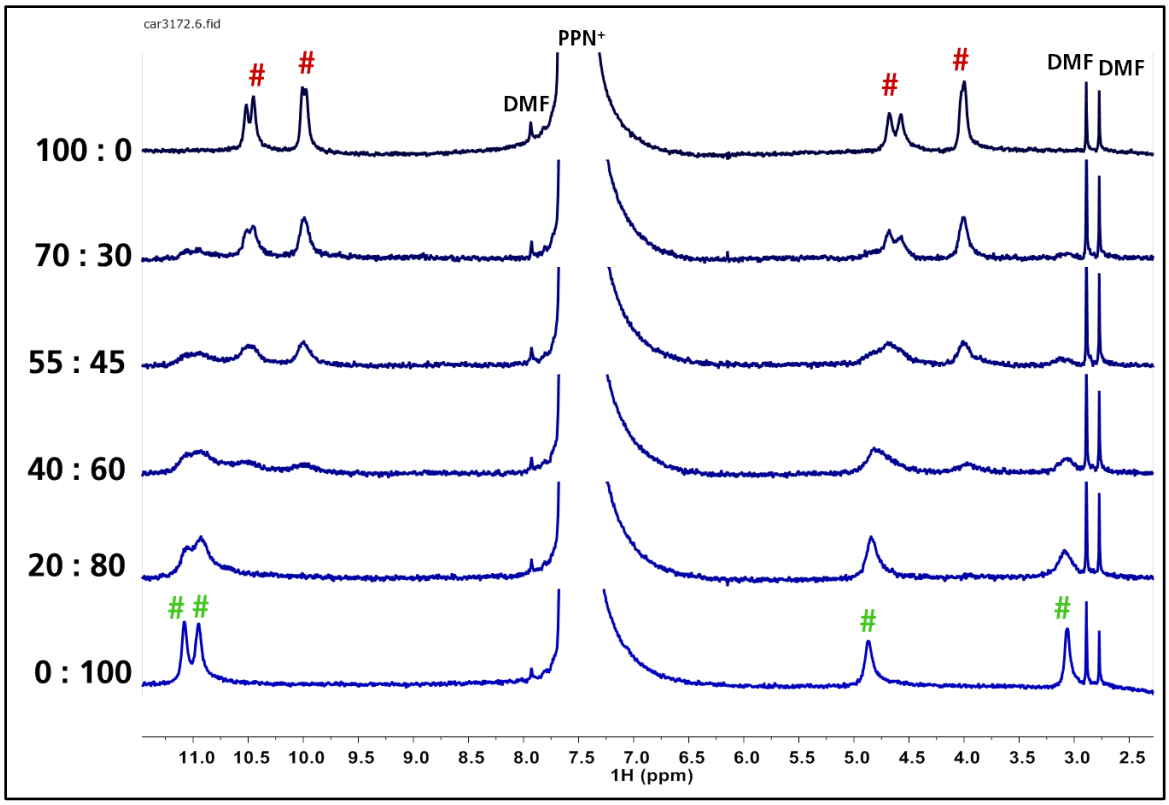

Figure S9. Stacked ^{1}H NMR spectra for 1.9 mM d_3-MeCN solutions of mixtures of di-ferric and mixed-valence $[Fe_2S_2(SArO)_2]^{2-/3-}$. The ratio of di-ferric to mixed-valence is indicated on the left. Peaks marked with a red # correspond to the di-ferric cluster, and those marked with a green # correspond to the mixed-valence congener.

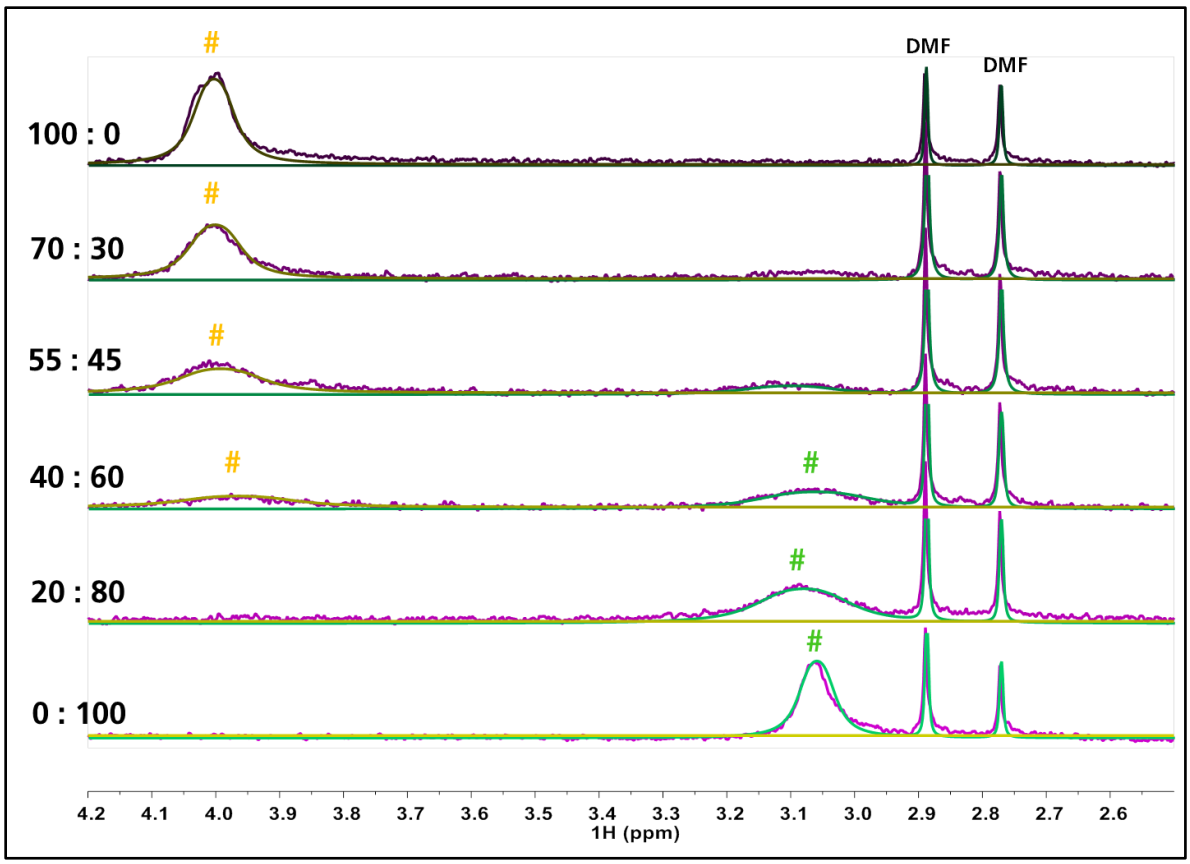

Figure S10. Overlay of stacked ^{1}H NMR spectra (experimental: purple; fit: gold or green) for 1.9 mM d_3-MeCN solutions of mixtures of di-ferric and mixed-valence $[Fe_2S_2(SArO)_2]^{2-/3-}$ (zoomed in from Figure S9). The ratio of di-ferric to mixed-valence is indicated on the left. Peaks marked with # were fit to a Lorentzian.

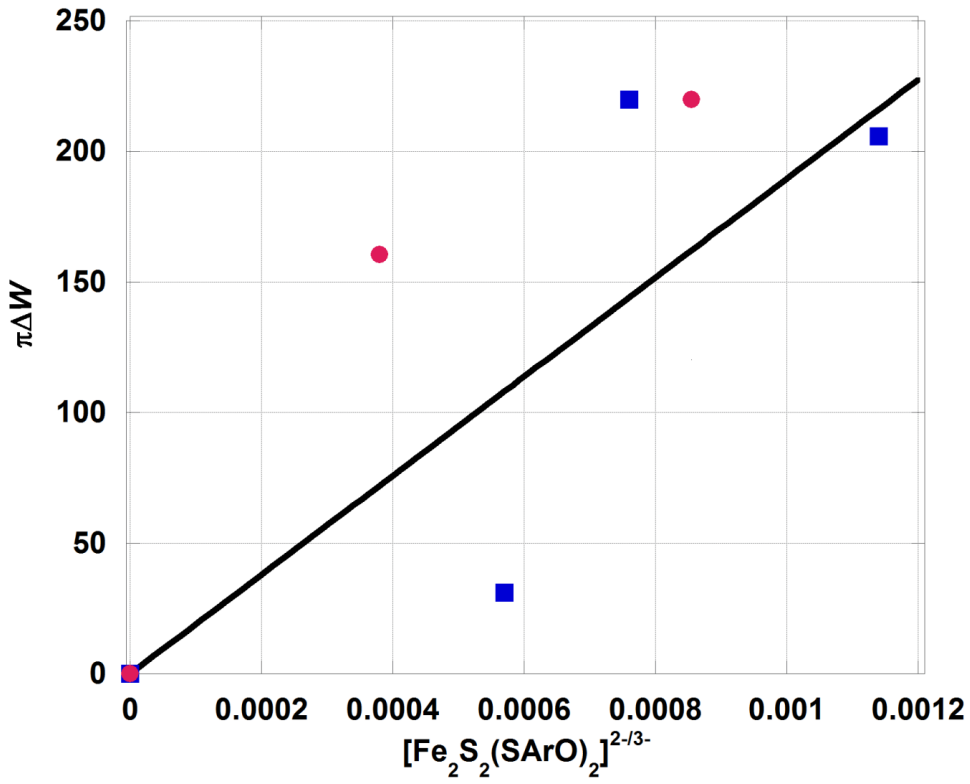

Figure S11. Plot of $\pi\Delta W$ vs. $[Fe_2S_2(SArO)_2]^{2-}$ (red circles) or $[Fe_2S_2(SArO)_2]^{3-}$ (blue squares). Blue squares correspond to changes in the line width of the di-ferric peak at 4.00 ppm upon addition of $[Fe_2S_2(SArO)_2]^{3-}$ and red circles correspond to changes in the line width of the mixed-valence peak at 3.06 ppm upon addition of $[Fe_2S_2(SArO)_2]^{2-}$. The rate constant for intermolecular ET was obtained from the linear fit of the data. From the slope, a rate constant of $(1.9 \pm 0.9) \times 10^5$ M^{-1} s^{-1} was obtained. The reported error is the standard deviation from fitting both datasets independently (to obtain k_5).

F.VI PCET Self-Exchange Kinetics for 1 and 4

Method 1: In the glove-box, solutions of **1** (2.0 mM), **2** (6.0 mM), and [DMAP-H]OTf (60 mM) were prepared in d_3-MeCN. 500 μL aliquots of the solution of **1** were transferred to four NMR tubes. To one tube, an additional 300 μL of d_3-MeCN was added. To a second tube, 100 μL of **2** and 440 μL of d_3-MeCN was added. To the third tube, 250 μL of **2** and 275 μL of d_3-MeCN was added. To the fourth tube, 500 μL of **2** and 0 μL of d_3-MeCN was added. The tubes were all capped with septa and parafilmed. The acid solution was transferred to a vial containing a septum screwcap which was then parafilmed. A 50 μL gas-tight syringe was inserted via the septum, as well as a 10 mL disposable syringe full of glove-box atmosphere (to keep the solution under inert atmosphere). The acid solution and NMR tubes were removed from the glove-box, and the samples frozen in a $MeCN/CO_2$ bath. The samples were removed from the cold bath and acid was added to the thawing solution (10, 25, and 50 μL to tubes 2, 3, and 4, respectively). The final concentrations of **1** for samples 2 – 4 was 0.95 mM, and the concentration of **2** was 0.57, 1.4, and 2.9 mM for samples 2 – 4. The concentration of **1** in

sample 1 was 1.4 mM (The linewidths do not change significantly with concentration). The samples were inverted twice, and frozen. Each sample was thawed, inserted into the chilled NMR probe, and allowed to thermally equilibrate in the probe for 5 minutes, after which the instrument was tuned and the shims adjusted. Spectra were collected at 243 K, and the data worked up as described above for ET kinetics (using the same peak). The reported error is the standard deviation.

Method 2: Mixtures of **1** and **4** were alternatively prepared by aliquoting solutions of **2**, ≤ 1 equiv TEMPO (both in d_3-MeCN), and d_3-MeCN into NMR tubes the glove-box. To these samples, 1 equiv of [DMAP-H]OTf (relative to **2**) was added as described above, to give samples containing mixtures of **1** and **4** (sample 1: 1.7 mM **1**; sample 2: 0.86 mM **1** and 0.86 mM **2**; sample 3: 0,07 mM **1** and 1.6 mM **4**). The data collection and work-up was likewise done as described above.

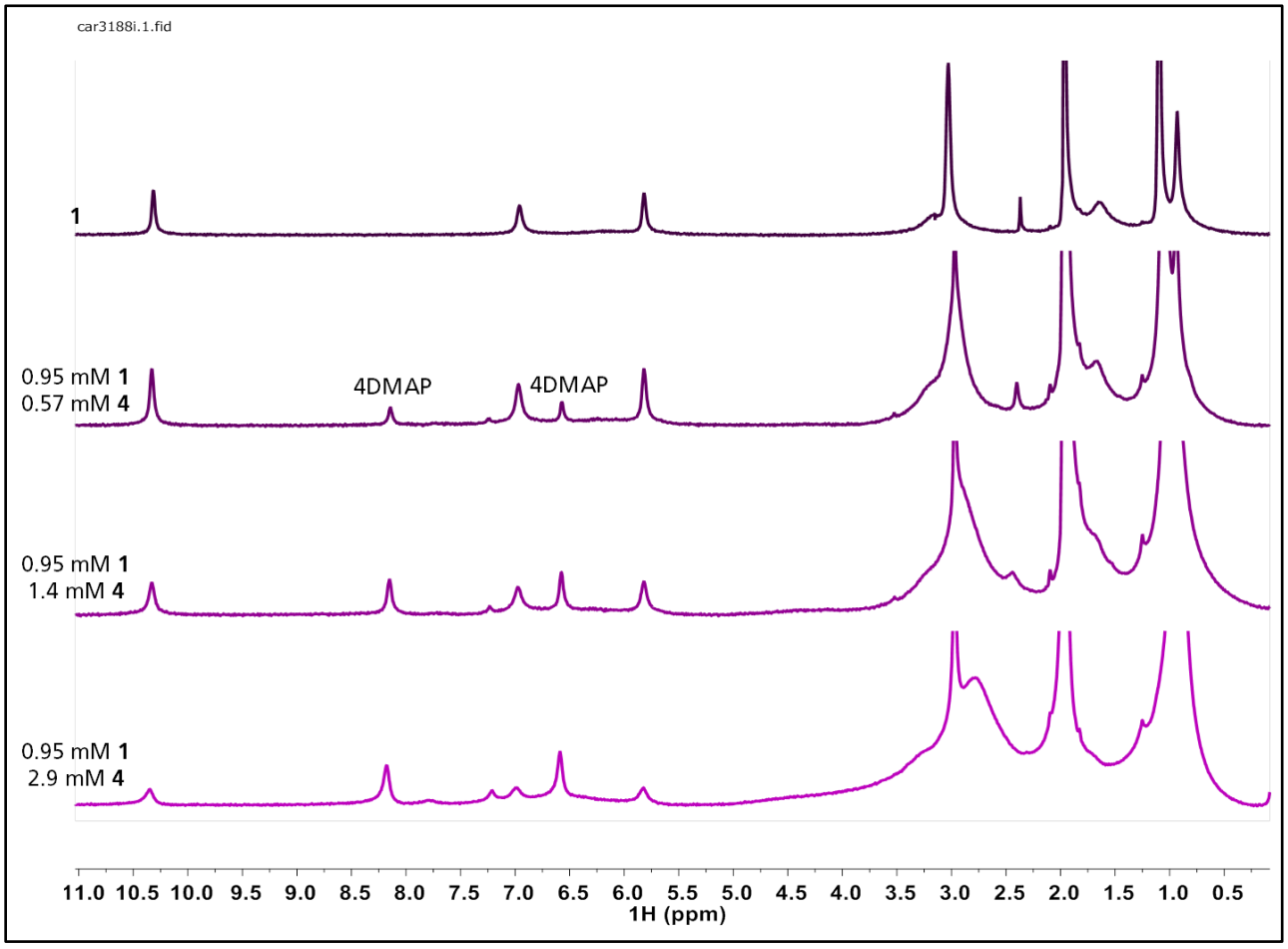

Figure S12. Overlay of stacked ^{1}H NMR spectra for mixtures of **1** and **4** in d_3-MeCN at -30 ^{o}C (method 1). The relative amounts of **1** to **4** are noted on the left.

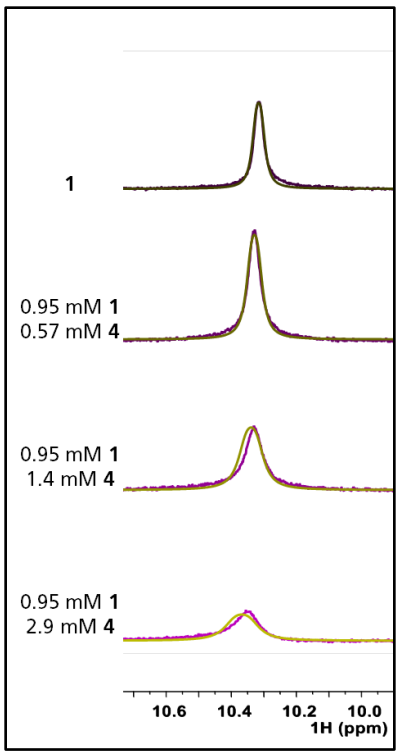

Figure S13. Overlay of stacked ^{1}H NMR spectra (experimental: purple; fit: gold) for d_3-MeCN solutions of mixtures of **1** and **4** (zoomed in from Figure S12). The ratio of **1** to **4** is indicated on the left.

G. Titration of 3 with TEMPOH (to give 5 + TEMPO)

Owing to the instability of the system, double-mixing stopped flow was employed for the titration. In the glove-box, MeCN solutions of **1** (0.51 mM), [DMAP-H]OTf (0.51 mM), and TEMPOH (2.5, 4.8, 6.4, and 10.8 mM) were prepared and transferred to syringes as described above.

Cluster **3** was prepared *in situ*, by mixing solutions of **1** and [DMAP-H]OTf. After a set delay time of 1 s, this solution was mixed with a solution of TEMPOH, and 100 UV-vis spectra were recorded (over the course of 15 - 60 seconds). The initial TEMPOH solution was diluted 2-fold, whereas the initial solution of **1** was diluted 4-fold. The spectrum of **3** was determined by mixing the solution of **3** (generated from the first mixing) with MeCN. The spectrum of **5** was determined by mixing a 0.51 mM solution of **2** with a 1.01 mM solution of [DMAP-H]OTf, and after a delay time of 0.01 s, mixing with MeCN. Three kinetic runs were done at each TEMPOH concentration. The UV-vis spectrum that corresponds to the equilibrium mixture was taken to be that at the time when the absorbances at 620 and 370 nm were at a minimum; the subsequent degradation reaction(s) result in increased absorption at these wavelengths (350 nm is an isosbestic point for the equilibration reaction). For the calculations described below, it is assumed that the subsequent degradation reaction has not commenced at this time. Using later time points does not substantially affect the final *K*. Because of the instability of **5**, the error

should increase with increasing TEMPOH concentrations. Owing to the large difference in the extinction coefficients for **3** and **5** at 524.7 nm, this wavelength was employed for the analysis described below.

The *K* was determined from the plot of [**5**][TEMPO]/[**3**] *vs.* [TEMPOH] (Figure S15). The concentrations of **5**, **3**, TEMPOH, and TEMPO were determined assuming mass balance as follows. At the wavelength monitored, the absorbance due to TEMPO and TEMPOH are negligible and hence excluded. Equation 1 defines the initial absorbance at a specific wavelength, prior to any addition of TEMPOH.

$$A_o = \varepsilon_{\mathbf{3}} b[\mathbf{3}]_o \tag{1}$$

Equation 2 defines the absorbance of **5**.

$$\mathrm{A_f} = \varepsilon_{\mathbf{5}} \mathrm{b}[\mathbf{5}]_\mathrm{f} \tag{2}$$

During the titration, the total concentration of iron is equal to the initial concentration of **3** and the final concentration of **5**, as described in equation 3. The subscript t denotes titration.

$$[\mathbf{5}]_\mathrm{f} = [\mathbf{3}]_\mathrm{o} = [\mathbf{3}]_\mathrm{t} + [\mathbf{5}]_\mathrm{t} \tag{3}$$

Likewise, the total concentration of TEMPOH/TEMPO at equilibrium is equal to the amount of TEMPOH added ($[\mathrm{TEMPOH}]_\mathrm{x}$), as described in equation 4 (mass-balance).

$$[\mathrm{TEMPOH}]_\mathrm{x} = [\mathrm{TEMPOH}]_\mathrm{t} + [\mathrm{TEMPO}]_\mathrm{t} \tag{4}$$

Assuming mass balance, the ratio of $[\mathbf{5}]_t/[\mathbf{3}]_t$ at a point in the titration can be described by equation 5.

$$\frac{\mathrm{A_t}-\mathrm{A_o}}{\mathrm{A_f}-\mathrm{A_t}} = \frac{\varepsilon_{\mathbf{3}} \mathrm{b}[\mathbf{3}]_\mathrm{t} + \varepsilon_{\mathbf{5}} \mathrm{b}[\mathbf{5}]_\mathrm{t} - \varepsilon_{\mathbf{3}} \mathrm{b}[\mathbf{3}]_\mathrm{o}}{\varepsilon_{\mathbf{5}} \mathrm{b}[\mathbf{5}]_\mathrm{f} - \varepsilon_{\mathbf{3}} \mathrm{b}[\mathbf{3}]_\mathrm{t} - \varepsilon_{\mathbf{5}} \mathrm{b}[\mathbf{5}]_\mathrm{t}} = \frac{\varepsilon_{\mathbf{3}}([\mathbf{3}]_\mathrm{t}-[\mathbf{3}]_\mathrm{o}) + \varepsilon_{\mathbf{5}}[\mathbf{5}]_\mathrm{t}}{\varepsilon_{\mathbf{5}}([\mathbf{5}]_\mathrm{f}-[\mathbf{5}]_\mathrm{t}) - \varepsilon_{\mathbf{3}}[\mathbf{3}]_\mathrm{t}} = \frac{\varepsilon_{\mathbf{5}}[\mathbf{5}]_\mathrm{t} - \varepsilon_{\mathbf{3}}[\mathbf{5}]_\mathrm{t}}{\varepsilon_{\mathbf{5}}[\mathbf{3}]_\mathrm{t} - \varepsilon_{\mathbf{3}}[\mathbf{3}]_\mathrm{t}} = \frac{[\mathbf{5}]_\mathrm{t}}{[\mathbf{3}]_\mathrm{t}} \tag{5}$$

Rearrangement of equation 5 gives equation 6.

$$[\mathbf{5}]_\mathrm{t} = [\mathbf{3}]_\mathrm{t} \frac{\mathrm{A_t}-\mathrm{A_o}}{\mathrm{A_f}-\mathrm{A_t}} \tag{6}$$

Combining equations 3 and 6 gives equation 7.

$$[\mathbf{5}]_\mathrm{t} = \frac{\frac{\mathrm{A_t}-\mathrm{A_o}}{\mathrm{A_f}-\mathrm{A_t}}[\mathbf{3}]_\mathrm{o}}{\frac{\mathrm{A_t}-\mathrm{A_o}}{\mathrm{A_f}-\mathrm{A_t}}+1} \tag{7}$$

At equilibrium, the concentration of **5** is equal to that of TEMPO (equation 8).

$$[\mathbf{5}]_\mathrm{t} = [\mathrm{TEMPO}]_\mathrm{t} \tag{8}$$

Combining equations 4 and 8 gives equation 9.

$$[\mathrm{TEMPOH}]_\mathrm{t} = [\mathrm{TEMPO}]_\mathrm{x} - [\mathbf{5}]_\mathrm{t} \tag{9}$$

The equilibrium constant is defined by equation 10.

$$K = \frac{[\mathbf{5}]_\mathrm{t}[\mathrm{TEMPO}]_\mathrm{t}}{[\mathbf{3}]_\mathrm{t}[\mathrm{TEMPOH}]_\mathrm{t}} \tag{10}$$

Equation 10 can be rearranged to give equation 11.

$$K[\mathrm{TEMPOH}]_t = \frac{[\mathbf{5}]_t[\mathrm{TEMPO}]_t}{[\mathbf{3}]_t} \quad (11)$$

Thus, a plot of $([\mathbf{5}]_t/[\mathbf{3}]_t)[\mathrm{TEMPO}]_t$ vs. [TEMPOH] gives *K*. These parameters are given by equations 5, 7, and 9. The BDFE of **5** is then obtained by equation 12.

$$\mathrm{BDFE}_{\mathbf{5}} = \mathrm{BDFE}_{\mathrm{TEMPOH}} + \mathrm{RTln}K \quad (12)$$

The BDFE of TEMPOH in MeCN is 66.5.[9]

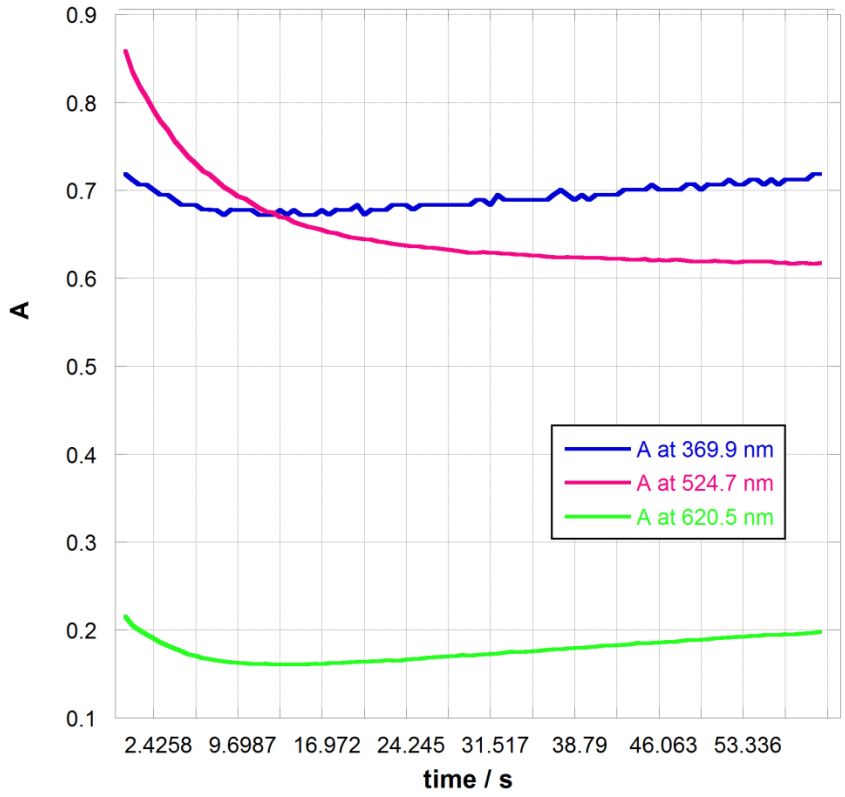

Figure S14. Exemplary plot of absorbance vs. time (at different wavelengths) for the equilibration of **3** + TEMPOH = **5** + TEMPO. Data is for mixing **3** with 4.8 mM of TEMPOH.

y = m1* M0		
	Value	Error
m1	0.01189	0.0014002
Chisq	6.5867e-11	NA
R	0.59224	NA

y = m1* M0		
	Value	Error
m1	0.01604	0.0028311
Chisq	2.6928e-10	NA
R	1	NA

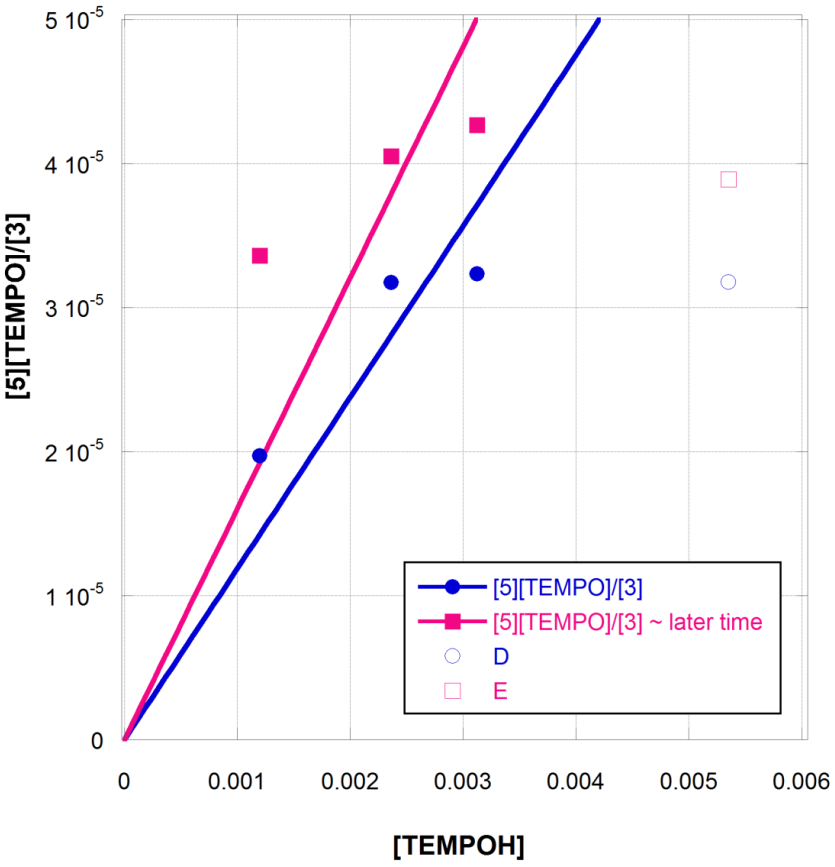

Figure S15. Plot of [**5**][TEMPO]/[**3**] vs. [TEMPOH]. The slope corresponds to *K*. Datapoints that are not shaded were omitted from the curve fitting. Inclusion of these points results in poorer fits, and slopes of 0.008 and 0.01 (blue and pink, respectively). Fitting to the first two points (lowest [TEMPOH]) improved the fits, and gave slopes of 0.014 and 0.019 (blue and pink, respectively). Blue points/line correspond to data obtained when the absorbances at 620 and 370 nm were at a minimum. Pink points/line correspond to absorbances measured at t = 60 s, when more degradation has occurred. The amount of degradation at this later time is different for each TEMPOH concentration.

From the plot shown in Figure S15, a value of 0.012 is obtained for *K*, which corresponds to a BDFE of 63.9 (± 0.9) kcal mol^{-1} for **5**. The error is from 3 x the range of *K*s obtained from the various line fittings.

H. Reactions of 4 and 5 with TEMPO

H.I Double Mixing Stopped-Flow Kinetics: Reaction of 4 with TEMPO

KIE determination: In the glove-box, MeCN solutions of **2** (0.50 mM), and TEMPO (3.0, 4.6, 7.4, and 10.9 mM) were prepared. Solutions of [DMAP-H]OTf and [DMAP-D]OTf (0.50 mM) were prepared in MeCN that contained 95 mM methanol or d_4-methanol (addition of d_4-methanol to a d_3-MeCN solution of **2** shows no degradation after ~ 15 minutes). Assuming 5 ppm H_2O in the MeCN, this corresponds to a 500-fold excess of exchangeable protons in the acid solution (125-fold excess in the reactions).

Cluster **4** was *prepared in situ*, by mixing solutions of **2** and [DMAP-H(D)]OTf. After a set delay time of 10 s, this solution was mixed with a solution of TEMPO, and 100 - 500 UV-vis spectra were recorded (over the course of 0.4 – 100 seconds). The initial TEMPO solution was diluted 2-fold, whereas the initial solution of **2** was diluted 4-fold. Four to six kinetic runs were done at each TEMPO concentration and temperature (-25, 0, 25, and 50 ^{o}C). Kinetic data were analyzed as described above.

Effect of ionic strength: In the glove-box, solutions of **2** (0.50 mM), TEMPO (2.2, 3.1, 6.7, and 7.8 mM), and [DMAP-H]OTf (0.50 mM) were prepared in MeCN that contained 0.1 M $^{n}Bu_4NPF_6$. Data collection (25 ^{o}C) and analysis was done as described above.

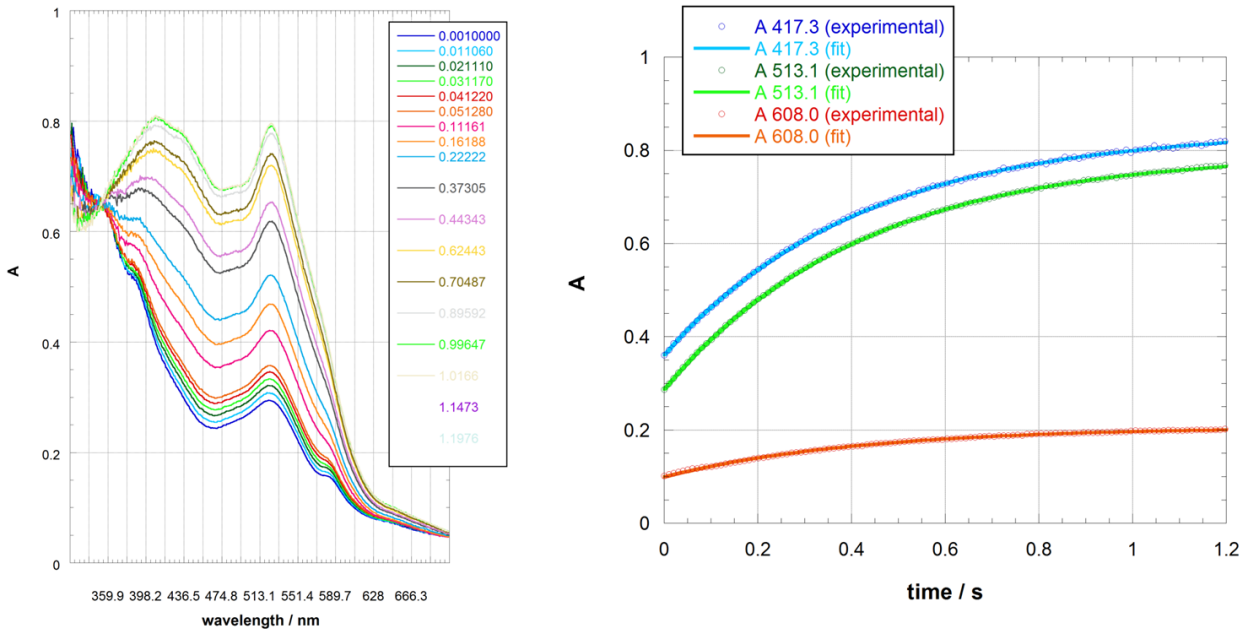

Figure S16. (left): Time evolution of UV-vis spectra of the reaction between *d*-**4** (0.13 mM; generated in the age-loop of the stopped-flow) and TEMPO (3.7 mM) over 1.2 s at 50 ^{o}C in MeCN. (right): Match between the experimental and *pseudo*-first-order fit resulting from Reactlab KINETICS global analysis over the whole wavelength region.

y = m1* M0		
	Value	Error
m1	141.53	1.566
Chisq	9.235	NA
R	0.97991	NA

y = m1* M0		
	Value	Error
m1	206.37	0.64641
Chisq	745.85	NA
R	0.96981	NA

y = m1* M0		
	Value	Error
m1	335.51	5.3211
Chisq	419.64	NA
R	0.82772	NA

y = m1* M0		
	Value	Error
m1	563.46	4.5584
Chisq	13.651	NA
R	0.98907	NA

y = m1* M0		
	Value	Error
m1	994.2	11.81
Chisq	5.2127	NA
R	0.99786	NA

y = m1* M0		
	Value	Error
m1	1675.9	22.365
Chisq	27.088	NA
R	0.98187	NA

y = m1* M0		
	Value	Error
m1	2478.3	16.616
Chisq	5.0809	NA
R	0.99924	NA

y = m1* M0		
	Value	Error
m1	3347.5	21.309
Chisq	1.9805	NA
R	0.99952	NA

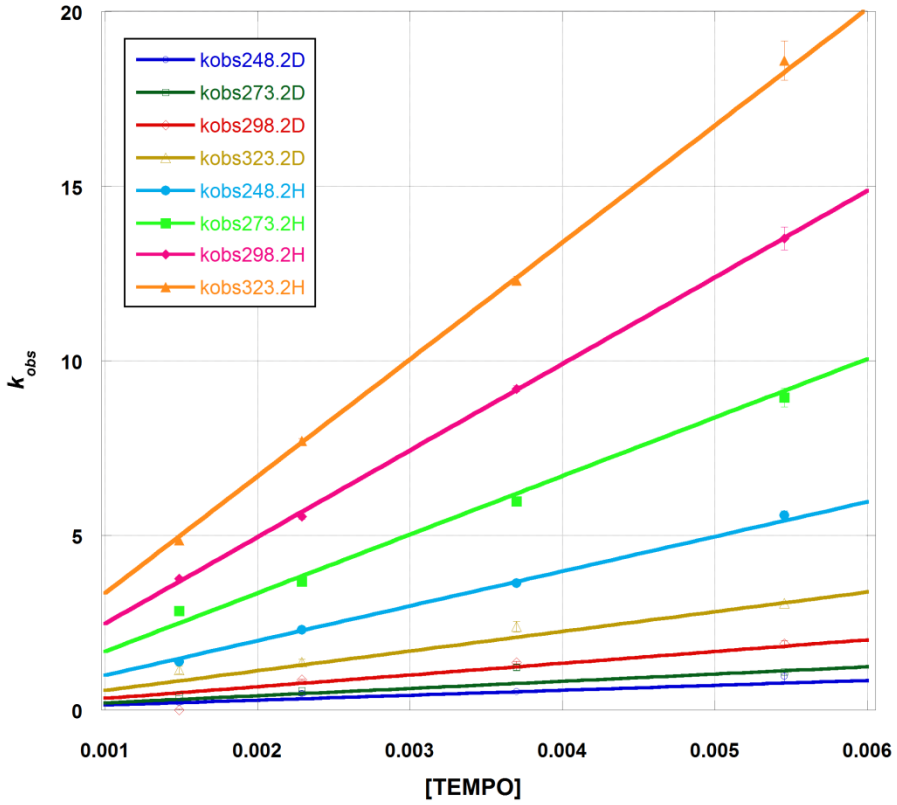

Figure S17. *Pseudo* first order plots of the reaction between **4** or *d*-**4** (0.13 mM, generated *in situ*) and excess TEMPO, obtained at different temperatures. The slope of each line gives the corresponding *k* for each temperature.

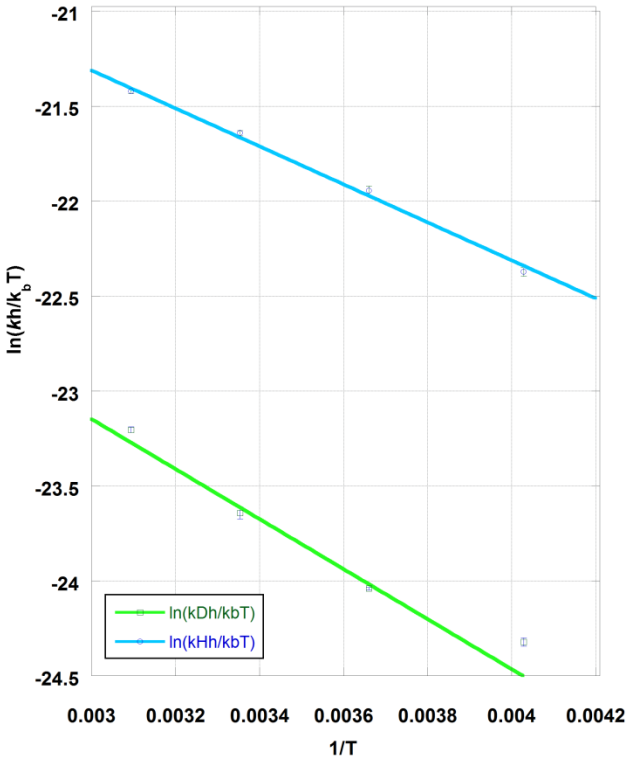

Figure S18. Eyring plot for the reaction of **4** and *d*-**4** with TEMPO. The following activation parameters are derived from the plot: $\Delta H^{\ddagger}_{H}$ = 1.99 ± 0.22 kcal mol^{-1}, $\Delta S^{\ddagger}_{H}$ = - 36.4 ± 1.4 cal K^{-1} mol^{-1}; $\Delta H^{\ddagger}_{D}$ = 2.62 ± 0.21 kcal mol^{-1}, $\Delta S^{\ddagger}_{D}$ = - 38.1 ± 1.6 cal K^{-1} mol^{-1}.

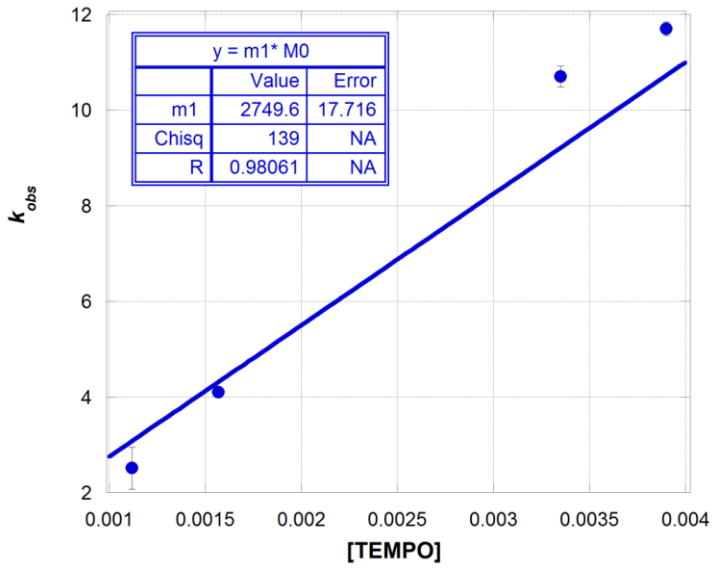

Figure S19. *Pseudo* first order plot of the reaction between **4** (0.13 mM, generated *in situ*) and excess TEMPO, in MeCN that contains 0.1 M $^{n}Bu_4NPF_6$.

H.2 Double Mixing Stopped-Flow Kinetics: Reaction of 5 with TEMPO

In the glove-box, MeCN solutions of **2** (0.50 mM), and TEMPO (2.6, 4.6, 7.2, and 10.6 mM) were prepared. Solutions of [DMAP-H]OTf and [4DMAPD]OTf (1.01 mM) were prepared in MeCN that contained 95 mM methanol or d_4-methanol. Cluster **5** was prepared *in situ*, by mixing solutions of **2** and [DMAP-H(D)]OTf. After a set delay time of 5 s, this solution was mixed with a solution of TEMPO, and 100 - 500 UV-vis spectra were recorded (over the course of 1.5 – 100 seconds). Four to six kinetic runs were done at each TEMPO concentration and temperature (-25, 0, 25, and 50 ^{o}C). Kinetic data were analyzed as described above. Fits of k_{obs} *vs.* [TEMPO] had non-zero intercepts, suggesting self-decomposition of **5**. Owing to the competing self-degradation, errors on the rate constants are reported as 3 x the standard deviation.

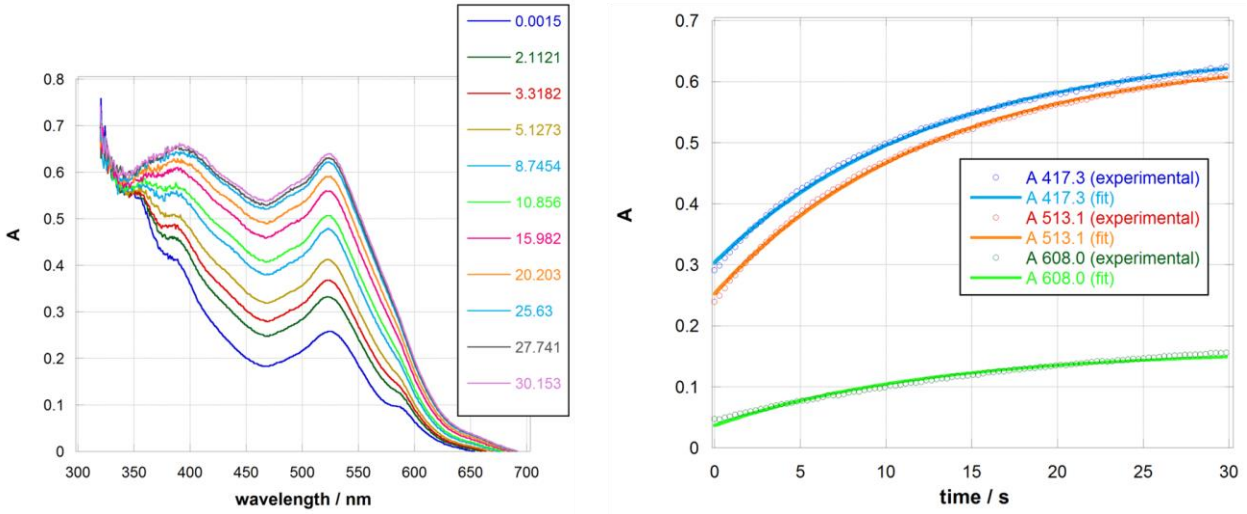

Figure S20. (left): Time evolution of UV-vis spectra of the reaction between *d*-**5** (0.13 mM; generated in the age-loop of the stopped-flow) and TEMPO (2.3 mM) over 30 s at 0 ^{o}C in MeCN. (right): Match between the experimental and *pseudo*-first-order fit resulting from Reactlab KINETICS global analysis over the whole wavelength region.

y = m1* M0+m2		
	Value	Error
m1	363.63	18.82
m2	0.29881	0.051569
Chisq	9.9128	NA
R	0.98698	NA

y = m1* M0+m2		
	Value	Error
m1	112.47	4.7667
m2	0.22133	0.024912
Chisq	11.895	NA
R	0.98949	NA

y = m1* M0		
	Value	Error
m1	126.67	1.767
Chisq	86.12	NA
R	0.96216	NA

y = m1* M0+m2		
	Value	Error
m1	28.976	20.813
m2	0.13884	0.035438
Chisq	1.2823	NA
R	0.77578	NA

y = m1* M0+m2		
	Value	Error
m1	104.95	3.9469
m2	0.33449	0.014232
Chisq	7.0619	NA
R	0.99504	NA

y = m1* M0+m2		
	Value	Error
m1	29.584	0.91324
m2	0.12765	0.0032838
Chisq	83.159	NA
R	0.96259	NA

y = m1* M0+m2		
	Value	Error
m1	12.663	2.9932
m2	0.048104	0.0071042
Chisq	21.204	NA
R	0.67655	NA

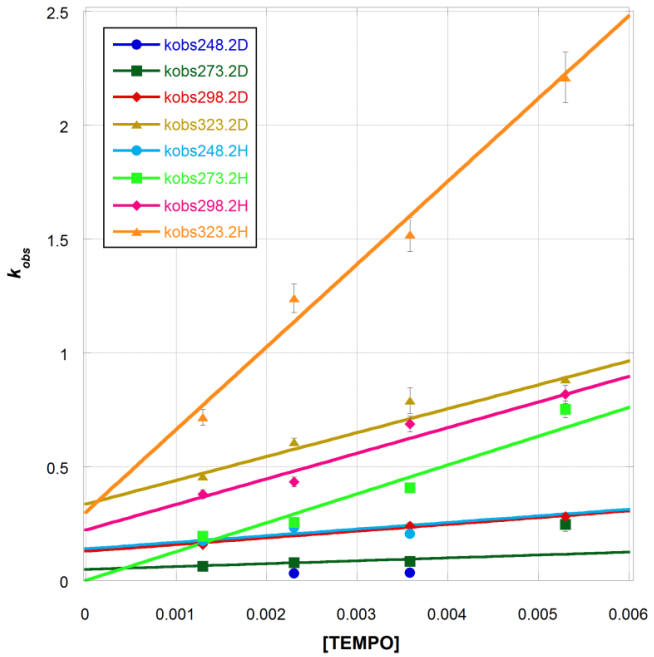

Figure S21. *Pseudo* first order plots of the reaction between **5** or *d*-**5** (0.13 mM, generated *in situ*) and excess TEMPO, obtained at different temperatures. The slope of each line gives the corresponding *k* for each temperature.

H.3 NMR Analysis of the Reaction of 5 with TEMPO

To a stirring solution of **2** (500 μL, 3.0 mM) in d_3-MeCN (that contained hexamethyldisiloxane as an internal standard), was added 2 equiv of [DMAP-H]OTf (100 μL, 30.0 mM in d_3-MeCN) via a 200 μL pipette. Immediately after the addition, 1 equiv of TEMPO (50 μL, 30.0 mM in d_3-MeCN) was added. An immediate color change from purple to red was noted. The reaction mixture was transferred to an NMR tube, and the resulting mixture analyzed ~ 15 minutes later. An NMR spectrum of the solution of **2** containing hexamethyldisiloxane was also obtained. Integration of peaks ascribed to **2** (control), **3** (reaction), and TEMPOH (reaction) relative to that of hexamethyldisiloxane gave yields of TEMPOH and **3**.

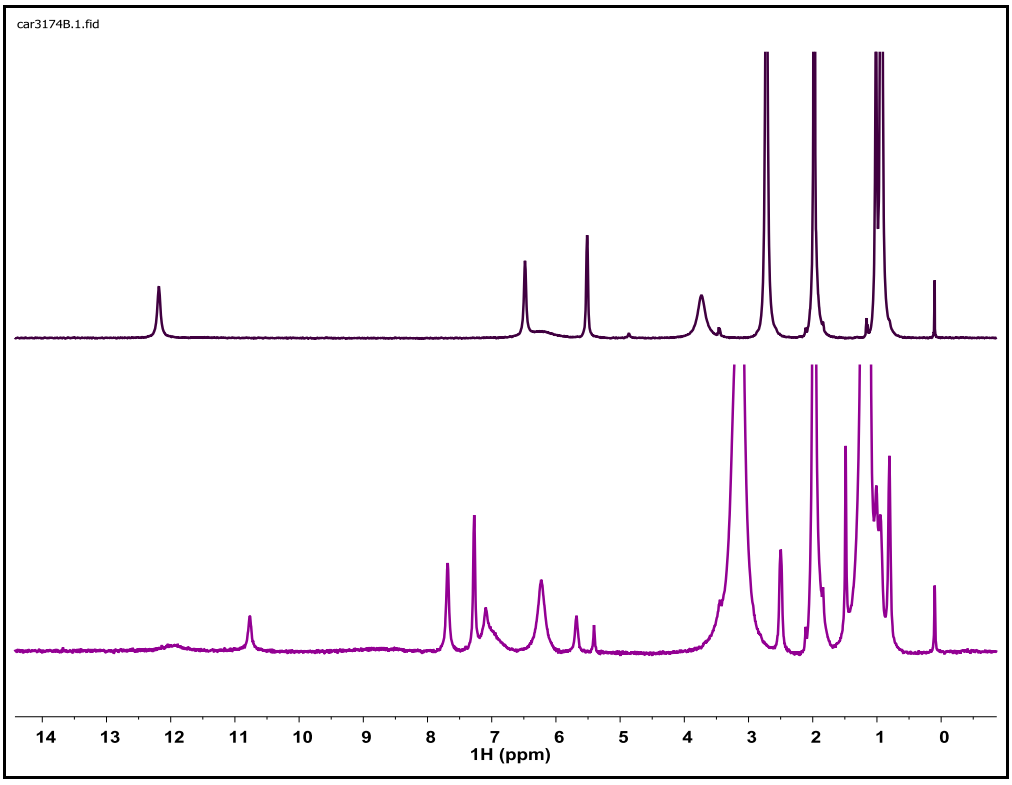

Figure S22. ^{1}H NMR spectra (d_3-MeCN) of (top): **2**; (bottom): the reaction of **5** (generated *in situ* from **2** and 2 equiv [DMAP-H]OTf) and TEMPO.

References

1 A. B. Pangborn, M. A. Giardello, R. H. Grubbs, R. K. Rosen and F. J. Timmers, *Organometallics*, 1996, **15**, 1518-1520.

2 F. Neese, *QCPE Bull.*, 1995, **15**, 5.

3 W. L. F. Armarego and C. L. L. Chai, *Purification of Laboratory Chemicals*, Butterworth-Heinmann, London, 2002.

4 E. A. Mader, A. S. Larsen and J. M. Mayer, *J. Am. Chem. Soc.*, 2004, **126**, 8066-8067.

5 C. T. Saouma, W. Kaminsky and J. M. Mayer, *J. Am. Chem. Soc.*, 2012, **134**, 7293-7296.

6 C. T. Saouma, W. Kaminsky and J. M. Mayer, *Polyhedron*, 2013, **58**, 60-64.

7 S. B. Harkins and J. C. Peters, *J. Am. Chem. Soc.*, 2004, **126**, 2885-2893.

8 J. Sandström, *Dynamic NMR Spectroscopy*, Academic Press Inc., New York, 1982.

9 J. J. Warren, T. A. Tronic and J. M. Mayer, *Chem. Rev.*, 2010, **110**, 6961-7001.